PRODUCTION OF NANOCOMPOSITES VIA EXTRUSION TECHNIQUES USING NANOPARTICLE CONTAINING DISPERSIONS AND THEIR MECHANICAL PROPERTIES

I. Hassinger[1*], T. Burkhart[1]

[1]*Institute for Composite Materials, Material Science, Technical University of Kaiserslautern, Erwin-Schrödinger-Straße, D-67663 Kaiserslautern, Germany*
**Irene.hassinger@ivw.uni-kl.de*

Keywords: Nanocomposites, nanoparticle dispersion, twin screw extrusion, mechanical properties.

Abstract
Nanoparticles are applied in polymer matrices because of building up an inorganic IPN network resulting in a simultaneous increase of stiffness and toughness provided that a good degree of nanoparticle dispersion with a very low amount of agglomerates can be realized. In order to prevent agglomerates, the incorporation of nanoparticle containing liquid dispersions into polymer matrices using appropriate extrusion technology is needed. SiO_2-nanoparticle containing dispersions were incorporated in polyamide 6 (PA 6) via twin screw extrusion using a special liquid feeding system. It is demonstrated that agglomeration of nanoparticles must be suppressed during the extrusion process, and that the nanoparticles have to cross over from the dispersing agent (water) to the polymer matrix melt in which they have to be well distributed. The respective feeding and extrusion technologies are presented in this paper. Additionally the resulting mechanical (tensile and Charpy impact) and morphological (SEM) properties of those nanocomposites are discussed. The impact strength could be slightly improved with strongly enhanced Young's modulus.

1 Introduction
Stiffness of thermoplastic polymers can be increased via reinforcement with microparticles but at the time impact and tensile strength are in most cases reduced. Nanoparticles however are in the position to increase stiffness, impact strength and tensile strength simultaneously [1]. The extraordinary properties of nanocomposites depend on their huge built-in interfacial surface area. Thus, the interface/interphase properties may become the dominant part of the macroscopic behavior of the nanoparticle-modified polymer composites, changing also the molecular mobility of polymer network. Furthermore, decreasing the particle size decreases also the average interparticle distance at constant volume fraction, leading to a potential network structure based on filler-filler interactions [2]. The effect of nanoparticles on mechanical properties depends on their dimensions, size, surface area, surface chemistry and interaction as well as distribution within polymer matrix. In case of low filler-matrix interaction, debonding occurs, which leads to microvoids as function of agglomerate size, where stresses can be concentrated. Only homogeneously distributed nanoparticles have the potential to increase the impact strength [1]. There are two different ways to produce

nanoparticle containing polymer nanocomposites: The most popular one is the deagglomeration of nanoparticle agglomerates by mechanical dispersion techniques in order to gain homogeneously distributed primary particles (top-down) [3-17], the other pathway is the bottom-up technique using in situ processes to produce nenoparticles e.g. sol-gel process [3,18]. Amongst the many different ways to produce particle-reinforced thermoplastics, the most important one is the continuous extrusion process [19]. Research has shown that shear energy input doing extrusion process is not sufficient to break up all the agglomerates not even when multiple extrusion processes are applied [20,21]. Thus, the incorporation of nanoparticle containing dispersions within extrusion process offers several advantages. The nanoparticles have to cross over from one media (dispersion) to another one (polymer). Nanoparticles for itself bear a potential health risk in form of a powder (top-down). The extent of the health damage risks cannot be estimated definitely, thus contamination with nanoparticle powder should be avoided. In case of bottom-up this kind of potential health risk will be avoided. In contrary to top-down where multiple extrusion steps have to be performed in case of bottom-up only a single extrusion step is necessary to distribute the already produced nanoparticles.

2 Materials and testing methods

2.1 Materials

In case of PA 6, Ultramid B 24 N 03 from BASF, a commercially available light stabilized polyamide 6 was used. The applied nanoparticle dispersions were on the one hand a commercially available SiO_2 containing dispersion with a mean particle size of 20 nm (Nanopol XP 20/0170 from Nanoresins GmbH) (Figure 1 a)). The filler content of the dispersion – in this paper called Nanopol - is 24.43 vol% (41.56 wt%). On the other hand a bottom-up spherical shaped SiO_2 nanoparticle containing dispersion was used. The particle size is 50 nm in water as dispersing agent (Figure 1 b)). This nanoparticle containing dispersion called SiO_2-Sol is produced via sol-gel technique in house with a particle concentration of 5.05 vol% (10.48 wt%). The respective pH-values of the two dispersions is 9-10.

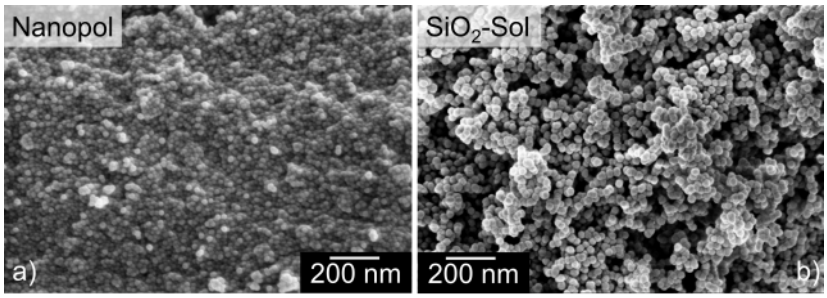

Figure 1. SiO_2 nanoparticles from the dried nanoparticle dispersion (a) Nanopol; b) SiO_2-Sol).

2.2 Extrusion

Before extrusion, PA 6 was dried for 24 h at 80°C. In case of extrusion, a co-rotating twin screw extruder from Berstorff GmbH was used. 6 kg/h of polymer was fed via high precision gravimetric feeder (K-tron Deutschland GmbH) and hopper to be processed at 250°C and 200 rpm. After the melting zone the nanoparticle containung dispersion is fed into the extruder cylinder via an excenter pump (type 3 RD 12-H from Viscotec GmbH, Germany). The water is extracted both via sidefeeder atmospherically and vacuum pump (Figure 2). The screw mainly consists of mixing elements (Figure 3).

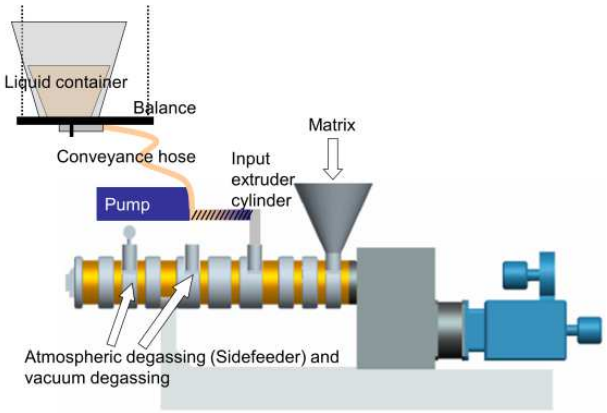

Figure 2. Build-up of the extrusion process with dispersion feeding in the extruder cylinder.

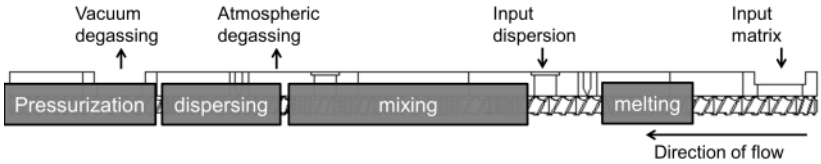

Figure 3. Screw design for adding nanoparticle dispersions within extrusion process.

As a reference we used PA6 extruded once with pure water in comparison to the respective PA6-nanocomposites. Table 1 gives an overview of the used dispersions applied in the respective extrusion.
The string resulted from a 4 mm die was cooled in a water bath, pelletized, dried and injection-molded (Allrounder 320, Arburg GmbH) to get test specimens for impact and tensile testing.

SiO_2 concentration in the resulting nanocomposite [vol%]	Used nanoparticle dispersion	Dispersion mass flow [kg/h]
-	-	0
-	Water	2.34
0.43	Nanopol	0.2
1.47	Nanopol	0.36
1.78	Nanopol	0.46
2.44	Nanopol	0.64
4.67	Nanopol	1.27
8.14	Nanopol	2.5
0.33	SiO_2-Sol	0.53
0.55	SiO_2-Sol	0.98
0.71	SiO_2-Sol	1.5
1.01	SiO_2-Sol	2.34
1.80	SiO_2-Sol	2.9

Table 1. SiO_2 PA6-nanocomposites with the end filler concentration produced from the given dispersions and the respective dispersion mass flow.

2.3 Charpy impact strength

Before mechanical testing the specimens were dried at 80°C for three days.
The Charpy notched bar impact strength was measured according to DIN EN ISO 179 on a pendulum-type impact testing machine (CEAST GmbH). The specimens were of type 1 with a notch of type A.

2.4 Tensile Tests
Before mechanical testing the specimens were dried at 80°C for three days.
Tensile tests were performed at room temperature on injection-molded specimens in accordance to DIN EN ISO 527-2 standard on a universal testing machine (Zwick GmbH model 1485).

2.5 Scanning Electron Microscopy (SEM) and analysis of dispersion index
Polished surfaces were analysed using an electron microscope (Supra 40 from Zeiss and JSM 6300 from Joel) via detecting the backscattering electrons. Fracture surfaces were scanned with a secondary electron detector. All samples were coated with gold using a Sputtering Device (SCD – 050, Balzer AG). The SEM-images were analysed with an image analysis software by which the number of agglomerates and size (for Nanopol > 1 µm; for SiO_2-Sol > 0.5 µm) were measured. From these results the dispersion index was calculated according to equation (1) [22]:

$$D = 1 - f \cdot \frac{A}{A_{im} \cdot \phi_{nano}} \qquad (1)$$

with
D ≙ dispersion index
A ≙ area of the agglomerates
A_{im} ≙ area of the image
f ≙ shape factor
Φ_{nano} ≙ volume fraction.

2.6 Definition of the shape factor
The shape factor f will be calculated with a so called control compound containing a well-defined dispersion of particles based on a defined volume content. Therefore, we used a nano reinforced PA 6 composite with no dispersion which will be set to zero regarding dispersion index. f can be calculated by solving the equation (2).

$$f = (1 - D) \cdot \frac{A_{im} \cdot \phi_{Nano}}{A} \qquad (2)$$

In our case f was set to 0.63.

2.7 Thermal properties
The filler content was analysed via thermo gravimetric analysis (TGA). The material was heated with 10 K/min from 40 to 550 °C, maintaining the temperature at 550 °C for 40 min.

3 Results and Discussion
Figure 4 represents the SEM image of with Nanopol filled PA6 containing 1.78 vol% SiO_2 nanoparticles. Figure 5 shows SEM images of PA6 filled with 1.80 vol% SiO_2-Sol particles produced via Sol-Gel. SiO_2-Sol builds up more agglomerates than Nanopol at same concentration range. Figure 6 shows the agglomerate area and agglomerate number for different size ranges. The SiO_2-Sol builds up more small agglomerates, whereas Nanopol builds up more big agglomerates. The lower the SiO_2-Sol filler concentration the better the dispersion quality (Figure 7). For nanoparticle concentrations lower than 1 vol% the SiO_2-Sol

shows a better dispersion index than Nanopol nanoparticles running through a maximum at 0.33 vol% with a dispersion index of maximum 0.66. Nanopol nanoparticles show a peak with a maximum dispersion index of 0.52 at 1.78 vol%.

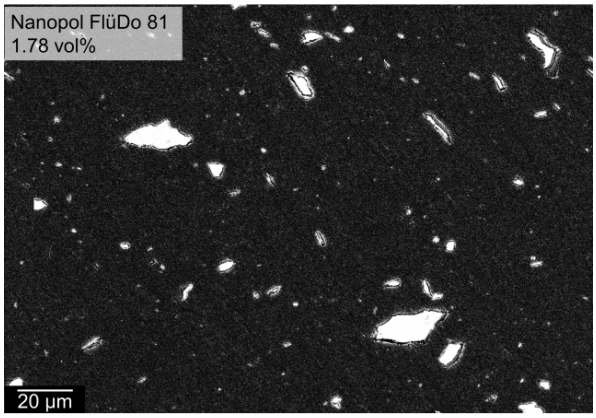

Figure 4. 1.78 vol% SiO_2 nanoparticle content in polyamide 6 from the incorporation of the Nanopol dispersion.

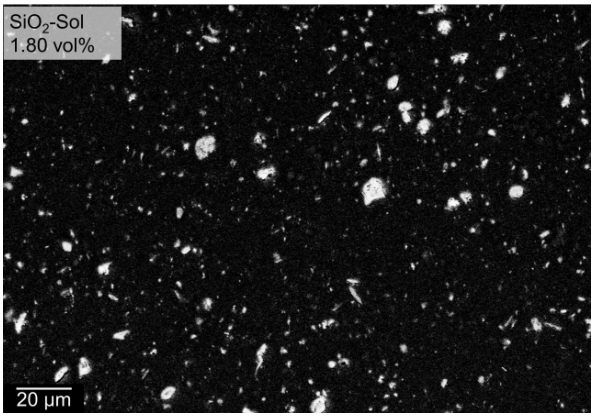

Figure 5. 1.80 vol% SiO_2 nanoparticle content in polyamide 6 from the incorporation of the SiO_2-Sol dispersion.

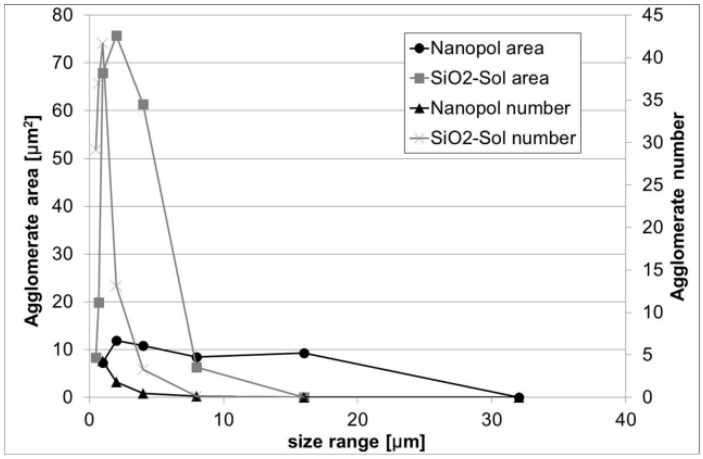

Figure 6. Agglomerate areas and agglomerate numbers in a certain size range for Nanopol and SiO_2-Sol filled PA6.

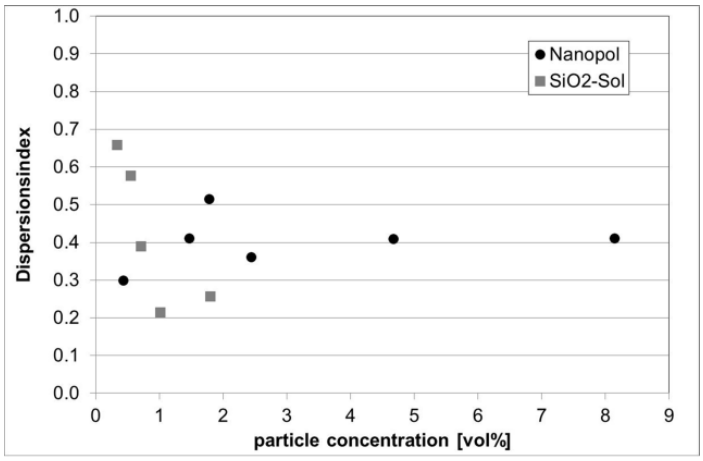

Figure 7. Dispersion index of Nanopol and SiO_2-Sol reinforced PA6 as a function of particle concentration.

Figure 8 represents the Charpy notched impact strength of the two different kinds of nanoparticles versus the particle concentration. Extruding of the virgin PA6 slightly increases impact strength. Incorporation of neat water in the polymer melt when extruding PA6 does not affect the impact strength. The impact strength will not be reduced through the

incorporation of neat water in the polymer melt. Incorporation of SiO_2 nanoparticles does not decrease the impact strength of the SiO_2-Sol filled nanocomposites for small amounts of SiO_2-Sol. A slight maximum of impact strength occurs at 0.55 vol%. At 0.7 vol% a severe decrease in impact strength starts, ending up at 1.8 vol% with 1.68 kJ/m^2, which is a total decrease of 37%. The Nanopol nanoparticles do also not generate an increase in impact strength, but the decrease as function of particle content is minor, having a strong decrease between 2.44 vol% and 4.67 vol%, ending up with a total decrease of 45%.

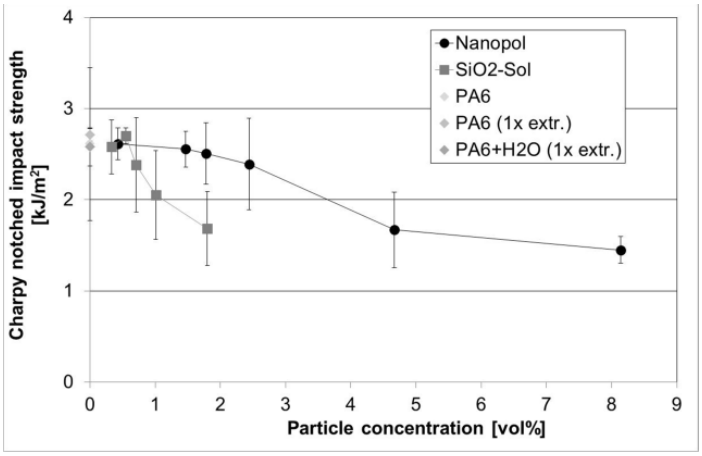

Figure 8. Charpy notched impact strength versus the particle content of Nanopol and SiO_2-Sol incorporated in PA6.

The extrusion and incorporation of water reduces the impact strength in the same amount it is increased by extrusion without water. The SiO_2-Sol nanoparticles generate a slightly higher impact strength for 0.55 vol% than for Nanopol nanoparticles having the same impact strength than once extruded neat PA6. Nanoparticles decrease the impact strength. As neat water incorporation does not show such a decrease, it is most probably the nanoparticles originating this decrease. The higher the nanoparticle concentration the higher is the probability of agglomeration (Figure 7) and thus leading to the observed reduction in impact strength. The Charpy impact strength is smaller for SiO_2 filled nanocomposites whose dispersion index is low as well. For Nanopol filled nanocomposites the dispersion index is increased and the Charpy impact strength is reduced less drastically.
The SiO_2-Sol and Nanopol nanoparticles show a similar particle-matrix interphase which can be seen in figure 9 and figure 10.

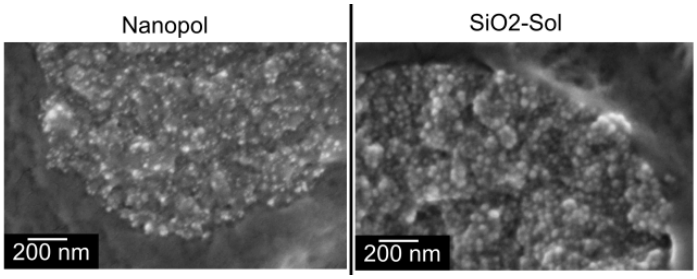

Figure 9. High resolution SEM image of a nanoparticle agglomerate (Nanopol and SiO_2-Sol) in PA6.

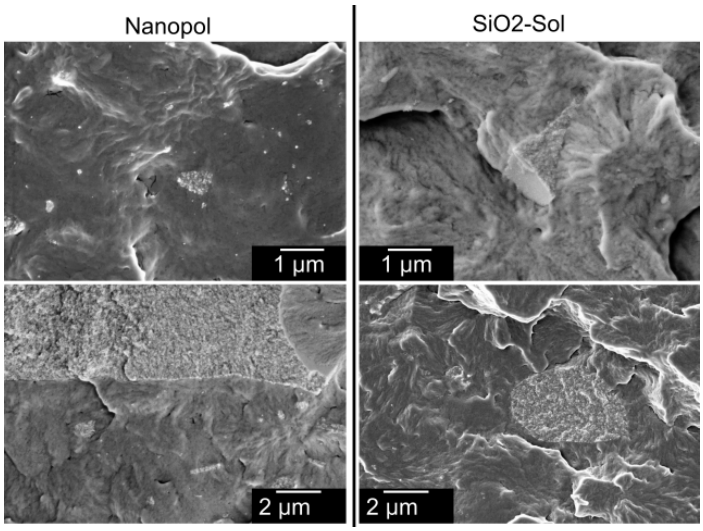

Figure 10. SiO_2-nanoparticle agglomerates of SiO_2-Sol and Nanopol particles embedded in a PA6 matrix. The agglomerate matrix interaction is good.

Figure 11-13 reveal the results of tensile tests. The Young's modulus (figure 11) is increased by extruding PA6 and by extruding PA6 with incorporation of water. The addition of nanoparticles increases the E-modulus linear by with rising filler content. For low filler grades we receive a local maximum at around 0.5 vol% for both types of nanoparticles. Their stiffening effect on the polymer seems to be independent of the nanoparticle type in this case.
The tensile strength (figure 12) is reduced by incorporation of nanoparticles. The SiO_2-Sol nanoparticles reinforce the material to a higher extent than Nanopol nanoparticles. Nanopol nanoparticles show a maximum in tensile strength at 2.44 vol%. SiO_2-Sol nanoparticles do not show a well-defined concentration dependency. Extrusion of PA6 with or without water does not influence the tensile strength. Again, we can except water as the dominant factor for the mechanical behaviour. The elongation at break (figure 13) is reduced dramatically by extruding and again by incorporation of water. The incorporation of nanoparticles decreases the elongation at break. But the SiO_2-Sol nanoparticles show a maximum of elongation at break at 0.55 vol%, Nanopol nanoparticles show a maximum at 2.44 vol% with a reduced elongation at break in comparison to neat PA6.

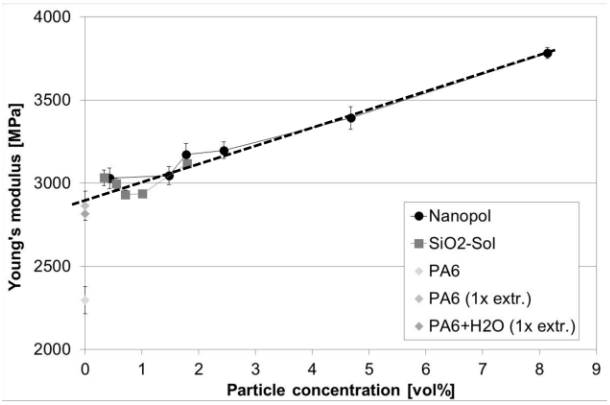

Figure 11. Young's modulus for Nanopol and SiO_2-Sol reinforced nanocomposites versus particle concentration. The reference is neat PA6, once extruded PA6, and once extruded PA6 including water.

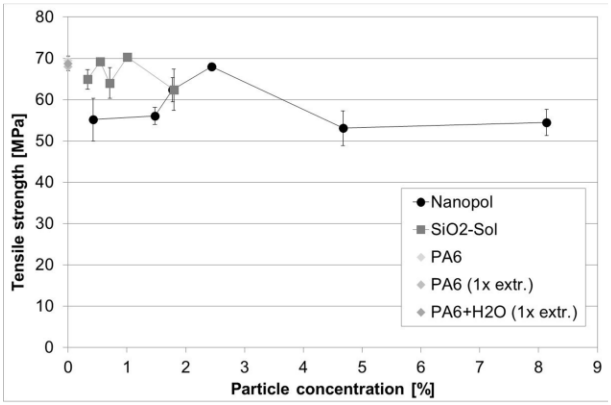

Figure 12. Tensile strength for Nanopol and SiO_2-Sol reinforced nanocomposites versus particle concentration. The reference is neat PA6, once extruded PA6 and once extruded PA6 including water.

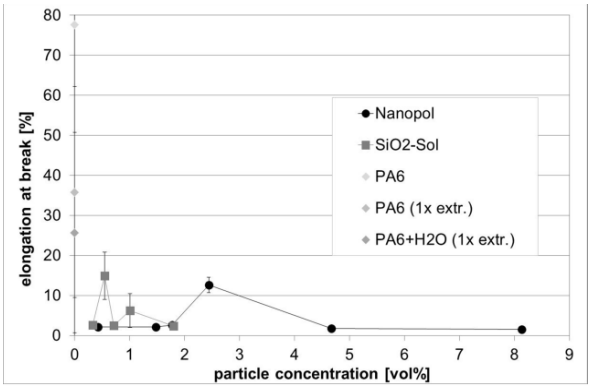

Figure 13. Elongation at break for Nanopol and SiO_2-Sol filled nanocomposites versus particle concentration. The reference is neat material, once extruded material and once extruded material including water.

4 Conclusion

Figure 14 reveals a net diagramm of the mechanical properties of the used references (neat PA6, PA6 once extruded, PA6 extruded with water) and figure 15 represents the results of the three nanoparticle filled PA6 nanocomposites (SiO_2-Sol (0.55 vol%) and Nanopol (0.43 vol%, 2.44 vol%)) in comparison to the neat PA6. Figure 14 demonstrates that the mechanical properties of the extruded PA6, with or without water, are on the same level or even better (Young's modulus) than the PA6 except for elongation at break. Figure 15 reveals that besides the elongation at break the SiO_2-Sol nanoparticles for low filler contents and the Nanopol nanoparticles for higher filler contents improve the mechanical properties of PA6 (Young's modulus) or sustain the level. For lower filler contents, however, Nanopol incorporation reduces the tensile strength and results in the lowest elongation at break.

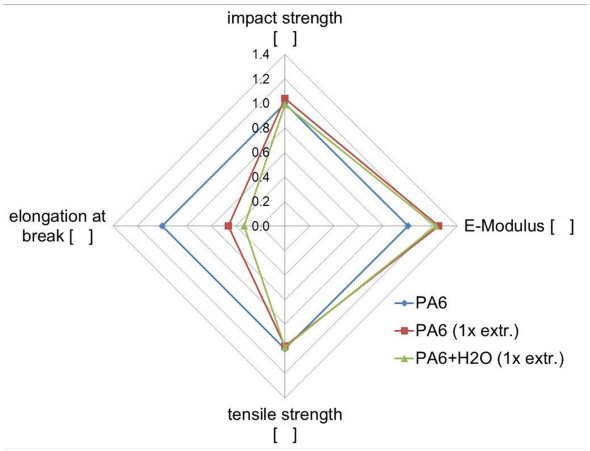

Figure 14. Summary of the mechanical data of the used references.

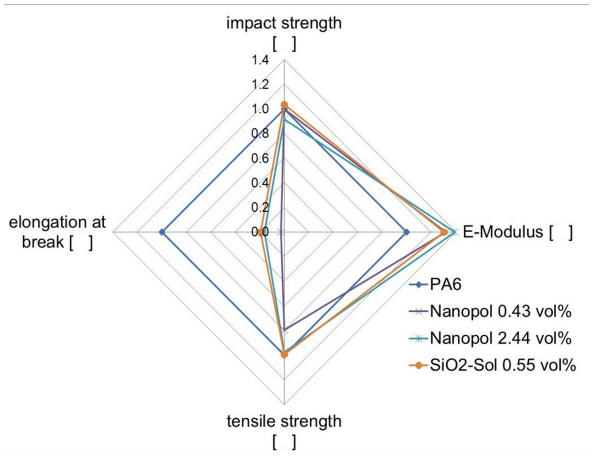

Figure 15. Summary of the mechanical data of the Nanopol reinforced PA6 (two concentrations) and of SiO_2-Sol reinforced PA6 (one concentration).

5 Acknowlegement

The authors gratefully acknowledge the financial support of the Federal German Ministry of Economics and Technology (BMWi) and the project management organization AIF Projekt GmbH for supporting this project included in the program Zentrales Innovationsprogramm Mittelstand (ZIM).

References

[1] Knör N., Schröck W., Haupert F., Schlarb A.K. *Innovative Nanoparticle Reinforced Thermoplastic Materials for Mechanical Applications* in "Proceeding of 2nd Vienna International Conference on Micro- and Nano-Technology", Vienna, Austria (2007).

[2] Ehrenstein G. W. *Polymer Werkstoffe*. 2 edition, Hanser publisher, Munich, Vienna (1999).

[3] Zhang M.Q., Rong M.Z., Friedrich K. *Processing and properties of nanolayered nanoparticle reinforced thermoplastic compositces* in "Handbook of Organic-Inorganic Hybrid Materials and Nanocomposites, Vol.2 Nanocomposites", edited by Nalwa H.S. American Scientific Publisher, Los Angeles, **2**, pp. 113-150 (2003).

[4] Komarneni S. Nanocomposites. *J. Mater. Chem*., **2,** pp. 1219-1230 (1992).

[5] Roy R. Purposive Design of Nanocomposites: Entire Class of New Materials. *Mater. Sci. Res.*, **21**, pp. 25-32 (1986).

[6] Dagani R. Nanostructured materials promise to advance range of technologies. *Chemical & Engineering News*, **23**, pp. 18-24 (1992).

[7] Rong M.Z., Zhang M.Q., Zheng Y.X., Walter R., Friedrich K. Structure-property relationships of irradiation grafted nano-inorganic particle filled polypropylene composites. *Polymer*, **42**, pp. 167-183 (2001).

[8] Rong M.Z., Zhang M.Q., Liu H., Zeng H.M. Synthesis of silver nanoparticles and their self-organization behavior in epoxy resin. *Polymer*, **40**, pp. 6169-6178 (1999).

[9] Van Bellingen C., Probst N., Grivei E. Specific conductive carbon blacks in plastics applications. *Polymer & Polymer Composites*, **10**, pp. 63-71 (2001).

[10] Chan C.M., Wu J., Li J.X., Cheung Y.K. Polypropylene/calcium carbonate nanocomposites. *Polymer*, **43**, pp. 2981-2992 (2002).

[11] Zilg C., Mülhaupt R., Finter J. Morphology and toughness/stiffness balance of nanocomposites based upon anhydride-cured epoxy resins and layered silicates. *Macromol. Chem. Phys.*, **200**, pp. 661-670 (1999).

[12] Ng C.B., Schadler L.S., Siegel R.W. Synthesis and mechanical properties of TiO2-epoxy nanocomposites. *Nanostructured Materials*, **12**, pp. 507-510 (1999).

[13] Riley A.M., Paynter C.D., McGenity P.M., Adams J.M. Factors affecting the impact properties of mineral filled polypropylene. *Plastics and Rubber Processing and Applications*, **14**, pp. 85-93 (1990).

[14] Ng, C.B., Ash, B.J., Schadler, L.S., Siegel, R.W. A study of the mechanical and permeability properties of nano- and micro-TiO2 filled epoxy composites. *Advanced Composites Letters*, **10**, pp. 101-111 (2001).

[15] Walter R., Friedrich K., Privalko V., Savadori A. On modulus and fracture toughness of rigid particulate filled HDPE. *Journal of Adhesion*, **64**, pp. 87-109 (1997).

[16] Levita G., Marchetti A., Lazzeri A. Fracture of Ultrafine Calcium Carbonate/Polypropylene Composites. *Polymer Composites*, **10**, pp. 39-43 (1989).

[17] Chan C-M., Wu J., Li J-X., Cheung Y-K. Polypropylene/calcium carbonate nanocomposites. *Polymer*, **43**, pp. 2981-2992 (2002).

[18] Brinker C. J., Scherer G. W. *Sol-Gel Science: The Physic and Chemistry of Sol-Gel Processing*, Elsevier Science, San Diego, London (1990).

[19] Rauwendaal C. *Polymer extrusion*. Hanser publisher, Munich, Vienna, New York, (1990).
[20] Knör N.F. *Einfluss der Verarbeitungstechnologie und Werkstoffzusammensetzung auf die Struktur-Eigenschafts-Beziehungen von thermoplastischen Nanoverbundwerkstoffen.* Vol. 93, Institut für Verbundwerkstoffe GmbH, Kaiserslautern (2010).
[21] Hassinger I., Burkhart T. Multiple extrusion and dilution of nanocomposites and their effect on the mechanical properties. *Journal of thermoplastic composite materials*, DOI: 10.1177/0892705711412646 (2011)
[22] Villmow T., Pötschke P., Pegel S., Häusler L., Kretzschmar B. Influence of twin-screw extrusion conditions on the dispersion of multi-walled carbon nanotubes in a poly(lactic acid) matrix. *Polymer,* **49**, pp. 3500–3509 (2008).